Voltammetric, Spectroscopic, and Microscopic Investigations of Electrocrystallized Forms of Semiconducting AgTCNQ (TCNQ = 7,7,8,8-Tetracyanoquinodimethane) Exhibiting Different Morphologies and Colors

Alexander R. Harris, Ayman Nafady,† Anthony P. O'Mullane, and Alan M. Bond*

School of Chemistry, Monash University, Clayton, Victoria, 3800, Australia

Received March 21, 2007. Revised Manuscript Received August 1, 2007

Chemically synthesized AgTCNQ exists in two forms that differ in their morphologies (needles and microcrystals) and colors (red and blue). It is now shown that both forms exhibit essentially indistinguishable X-ray diffraction, spectroscopic, and thermochemical data, implying that they are not separate phases, as implied in some literature. Electrochemical reduction of $TCNQ_{(MeCN)}$ in the presence of $Ag^{+}_{(MeCN)}$ generates both red and blue AgTCNQ. On glassy carbon, platinum, or indium tin oxide electrodes and at relatively positive deposition potentials, slow growth of high aspect ratio, red needle AgTCNQ crystals occurs. After longer times and at more negative deposition potentials, blue microcrystalline AgTCNQ thin films are favored. Blue AgTCNQ is postulated to be generated via reduction of a $Ag^{+}[(TCNQ^{\bullet-})(TCNQ)]_{(MeCN)}$ intermediate. At even more negative potentials, $Ag_{(metal)}$ formation inhibits further growth of AgTCNQ. On a gold electrode, $Ag_{(metal)}$ deposition occurs at more positive potentials than on the other electrode materials examined. However, surface plasmon resonance data indicate that a small potential region is available between the stripping of $Ag_{(metal)}$ and the oxidation of $TCNQ^{\bullet-}_{(MeCN)}$ back to $TCNQ_{(MeCN)}$ where AgTCNQ may form. AgTCNQ in both the red and blue forms also can be prepared electrochemically on a $TCNQ_{(s)}$ modified electrode in 0.1 M $AgNO_{3(aq)}$ where deposition of $Ag_{(metal)}$ onto the $TCNQ_{(s)}$ crystals allows a charge transfer process to occur. However, the morphology formed in this solid−solid phase transformation is more difficult to control.

Introduction

TCNQ (7,7,8,8-tetracyanoquinodimethane) based charge transfer salts have been of significant interest for several decades due to their high conductivity,[1] electrical switching properties,[2−9] and their use in sensing and other applications.[10−12] Both CuTCNQ and AgTCNQ, which is of interest in this paper, undergo electrical switching from a low to high conductivity state when subjected to an optical or electrical field. However, the conductivity of AgTCNQ is significantly lower (1.25×10^{-6} S cm^{-1}) than that of both CuTCNQ phases (0.25 and 1.3×10^{-5} S cm^{-1}).[1,13,14]

Publications related to AgTCNQ contain many methods of synthesis that claim to produce different crystal morphologies and film thicknesses on substrates. These include dipping a silver metal film into a solution of $TCNQ_{(MeCN)}$,[15] precipitation of $Ag^{+}_{(MeCN)}$ with $TCNQ^{\bullet-}_{(MeCN)}$ in acetonitrile,[1] vapor deposition[5] and incorporation into Langmuir−Blodgett films.[16] In 1985, electrocrystallization was performed in a two electrode cell from $Ag_{(metal)}$ and $TCNQ_{(MeCN)}$ by holding the electrode potential difference at 500 mV. This experiment produced red crystals[17] as opposed to the blue crystals seen in the original synthetic method.[1] Another electrocrystallization study was said to generate a charge transfer salt, designated as Ag_4TCNQ_3, although no hard data appear to be available to substantiate this formulation.[18] A later infrared and Raman spectroscopic investigation of five different

* Author to whom correspondence should be addressed. E-mail: alan.bond@sci.monash.edu.au.

† Permanent address: Chemistry Department, Faculty of Science, Sohag University, Sohag, Egypt.

(1) Melby, L. R.; Harder, R. J.; Hertler, W. R.; Mahler, W.; Benson, R. E.; Mochel, W. E. *J. Am. Chem. Soc.* **1962**, *84*, 3374−87.
(2) Potember, R. S.; Poehler, T. O.; Cowan, D. O. *Appl. Phys. Lett.* **1979**, *34*, 405−407.
(3) Potember, R. S.; Poehler, T. O.; Cowan, D. O.; Bloch, A. N. *NATO ASI Ser., Ser. C* **1980**, *56*, 419−28.
(4) Potember, R. S.; Poehler, T. O.; Benson, R. C. *Appl. Phys. Lett.* **1982** *41*, 548−550.
(5) Kamitsos, E. I.; Risen, J., W. M. *Solid State Commun.* **1983**, *45*, 165−169.
(6) Benson, R. C.; Hoffman, R. C.; Potember, R. S.; Bourkoff, E.; Poehler, T. O. *Appl. Phys. Lett.* **1983**, *42*, 855−7.
(7) Poehler, T. O.; Potember, R. S.; Hoffman, R.; Benson, R. C. *Mol. Cryst. Liq. Cryst.* **1984**, *107*, 91−101.
(8) Kamitsos, E. I.; Risen, W. M., Jr. *Mol. Cryst. Liq. Cryst.* **1986**, *134*, 31−42.
(9) Potember, R. S.; Poehler, T. O.; Rappa, A.; Cowan, D. O.; Bloch, A. N. *Synth. Met.* **1982**, *4*, 371−80.
(10) Sharp, M.; Johansson, G. *Anal. Chim. Acta* **1971**, *54*, 13−21.
(11) Wooster, T. J.; Bond, A. M. *Analyst* **2003**, *128*, 1386−1390.
(12) Wooster, T. J.; Bond, A. M.; Honeychurch, M. J. *Anal. Chem.* **2003**, *75*, 586−592.
(13) Yamaguchi, S.; Viands, C. A.; Potember, R. S. *J. Vac. Sci. Technol., B* **1991**, *9*, 1129−33.
(14) Heintz, R. A.; Zhao, H.; Ouyang, X.; Grandinetti, G.; Cowen, J.; Dunbar, K. R. *Inorg. Chem.* **1999**, *38*, 144−156.
(15) Cao, G.; Ye, C.; Fang, F.; Xing, X.; Xu, H.; Sun, D.; Chen, G. *Mater. Sci. Eng., B* **2005**, *B119*, 41−45.
(16) Yuan, C. W.; Wu, C. R.; Wei, Y.; Yang, W. Y. *Thin Solid Films* **1994**, *243*, 679−82.
(17) Shields, L. *J. Chem. Soc., Faraday Trans. 2* **1985**, *81*, 1−9.
(18) Kathirgamanathan, P.; Rosseinsky, D. R. *Chem. Commun.* **1980**, 839−40.

10.1021/cm070780b CCC: $37.00
Published on Web 10/23/2007

synthetic routes,[19] including both electrocrystallization methods, was undertaken to obtain a greater understanding of Ag(I)-TCNQ charge transfer salts. All the synthetic methods were concluded to produce a 1:1 AgTCNQ moiety, and nothing suggested the existence of the proposed Ag_4TCNQ_3 formulation.[18]

There has been considerable renewed interest in CuTCNQ and AgTCNQ, since the discovery that CuTCNQ, and possibly AgTCNQ, could be chemically synthesized in two distinct phases.[14,20] However, unlike the case with CuTCNQ, no single-crystal X-ray data are available to distinguish the two proposed blue and red AgTCNQ phases, and both exhibit identical Raman and infrared spectroscopic bands.[19]

The synthetic routes reported for the two proposed forms of AgTCNQ are distinctly different.[20] Blue, microcrystalline, so-called phase I was prepared by the reaction of LiTCNQ with $Ag^+_{(MeCN)}$ in acetonitrile, whereas so-called phase II, red needles were prepared by reaction of $TCNQ_{(MeCN)}$ and $Ag_{(metal)}$. Impure phase II was also said to be prepared by refluxing phase I AgTCNQ in acetonitrile over several days. These reaction pathways suggest that methods[21−26] used to control crystal morphology of electrochemically synthesized CuTCNQ in acetonitrile may be applied to the AgTCNQ system. In one approach, reducing $TCNQ_{(MeCN)}$ (eq 1) in the presence of $Ag^+_{(MeCN)}$, if it follows the chemical route, should allow the electrocrystallization of blue AgTCNQ (eq 2). Alternatively, electrochemical reduction of $Ag^+_{(MeCN)}$ to $Ag_{(metal)}$ (eq 3) in the presence of $TCNQ_{(MeCN)}$ should mimic the published chemical synthetic route and favor formation of red AgTCNQ (eq 4). However, achievement of separated pathways requires that the potentials for the $TCNQ^{0/\bullet -}$ and $Ag^{+/0}$ reduction processes allow avoidance of the situation where $TCNQ_{(MeCN)}$ and $Ag^+_{(MeCN)}$ are simultaneously reduced to $TCNQ^{\bullet -}_{(MeCN)}$ and $Ag_{(metal)}$ respectively.

$$TCNQ_{(MeCN)} + e^- \rightleftharpoons TCNQ^{\bullet -}_{(MeCN)} \quad (1)$$

$$TCNQ^{\bullet -}_{(MeCN)} + Ag^+_{(MeCN)} \overset{\text{precipitation}}{\rightleftharpoons} [Ag^+TCNQ^{\bullet -}]_{(s)} \quad (2)$$

$$Ag^+_{(MeCN)} + e^- \rightleftharpoons Ag_{(metal)} \quad (3)$$

$$Ag_{(metal)} + TCNQ_{(MeCN)} \overset{\text{precipitation}}{\rightleftharpoons} [Ag^+TCNQ^{\bullet -}]_{(s)} \quad (4)$$

In principle AgTCNQ also may be formed electrochemically by a solid−solid redox conversion process when water immiscible $TCNQ_{(s)}$ is adhered to an electrode surface which is placed in contact with an aqueous solution of 0.1 M $AgNO_{3(aq)}$. However, no literature is available to predict whether the red or blue phase forms might be produced, under these conditions.

In this paper we apply a range of electrochemical and other techniques to study the formation of AgTCNQ in acetonitrile and water. We also characterize the electrochemically generated solids formed on the electrode surfaces via microscopic, spectroscopic, and X-ray diffraction methods and surface plasmon resonance. Intriguingly, while we find that electrochemical formation of morphologically different blue and red crystals of AgTCNQ does occur, XRD, spectroscopic and thermochemical data obtained from either form are experimentally indistinguishable. This observation leads us to query whether crystals of different morphology rather than two phases are formed with the AgTCNQ system.

Experimental Section

Chemicals. 98% tetrakis(acetonitrile) silver(I) tetrafluoroborate ($[Ag(MeCN)_4]BF_4$), 98% TCNQ, KNO_3, and ferrocenemethanol from Aldrich; silver nitrate from Analar; 99.99% acetonitrile from Omnisolv; water (18.2 MΩ cm, Sartorius water purification system) and electrochemical grade tetrabutylammonium tetrafluoroborate (Bu_4NBF_4) used as an electrolyte (Sachem) in electrochemical studies were used as provided by the manufacturer.

Instrumentation and Procedures. Voltammetric instrumentation, cells and electrodes (working, reference, and auxiliary), and procedures were as described elsewhere.[22−25,27,28] TCNQ or AgTCNQ modified electrodes were prepared by placing crystals onto weighing paper and grinding them onto the electrode surface (mechanical attachment method) or by dissolving TCNQ in acetonitrile, pipetting a small volume of the solution onto the electrode surface, and allowing the solvent to evaporate (drop cast method).

Instrumentation and procedures used for the following techniques also are as described elsewhere: surface plasmon resonance (SPR);[25] scanning electrochemical microscopy (SECM);[23] scanning electron microscopy (SEM);[22] optical imaging;[24] electronic spectroscopy;[22] diffuse reflectance infrared Fourier transform spectroscopy (DRIFT),[22] and Raman spectroscopy.[28] X-ray powder diffraction (XRD) patterns of electrocrystallized AgTCNQ removed from a GC electrode (solvent and electrolyte removed) were obtained at 40 kV and 25 mA (Philips). Scans were from 2 to 60° (in steps of 0.02° at 2 s per step) with a divergence slit of 1° and a receiving slit of 0.2° using a graphite monochromator. Differential scanning calorimetry (DSC) over a temperature range of −150 to 370 °C was carried out on a Perkin-Elmer Q100 instrument at a scanning rate of 10 °C min^{-1}.

Results and Discussion

Characterization of AgTCNQ, in So-Called Phase I and II Forms, When Synthesized by Published Chemical Methods. AgTCNQ, in the so-called phase I and II forms, was synthesized according to ref 20. In agreement with this study, so-called phase I was a blue microcrystalline material (Figures 1a and c) while so-called phase II was detected as red needles of very high aspect ratio, some appearing to be

(19) Kamitsos, E. I. *Mol. Cryst. Liq. Cryst.* **1988**, *161*, 335−46.
(20) O'Kane, S. A.; Clerac, R.; Zhao, H.; Ouyang, X.; Galan-Mascaros, J. R.; Heintz, R.; Dunbar, K. R. *J. Solid State Chem.* **2000**, *152*, 159−173.
(21) Neufeld, A. K.; Madsen, I.; Bond, A. M.; Hogan, C. F. *Chem. Mater.* **2003**, *15*, 3573−3585.
(22) Harris, A. R.; Neufeld, A. K.; O'Mullane, A. P.; Bond, A. M.; Morrison, R. J. S. *J. Electrochem. Soc.* **2005**, *152*, C577−C583.
(23) O'Mullane, A. P.; Neufeld, A. K.; Bond, A. M. *Anal. Chem.* **2005**, *77*, 5447−5452.
(24) O'Mullane, A. P.; Neufeld, A. K.; Harris, A. R.; Bond, A. M. *Langmuir* **2006**, *22*, 10499−10505.
(25) Harris, A. R.; Neufeld, A. K.; O'Mullane, A. P.; Bond, A. M. *J. Mater. Chem.* **2006**, *16*, 4397−4406.
(26) Neufeld, A. K.; O'Mullane, A. P.; Bond, A. M. *J. Am. Chem. Soc.* **2005**, *127*, 13846 -13853.
(27) Nafady, A.; O'Mullane, A. P.; Bond, A. M.; Neufeld, A. K. *Chem. Mater.* **2006**, *18*, 4375−4384.
(28) Nafady, A.; Bond, A. M.; Bilyk, A.; Harris, A. R.; Bhatt, A. I.; O'Mullane, A. P.; De Marco, R. *J. Am. Chem. Soc.* **2007**, *129*, 2369−2382.

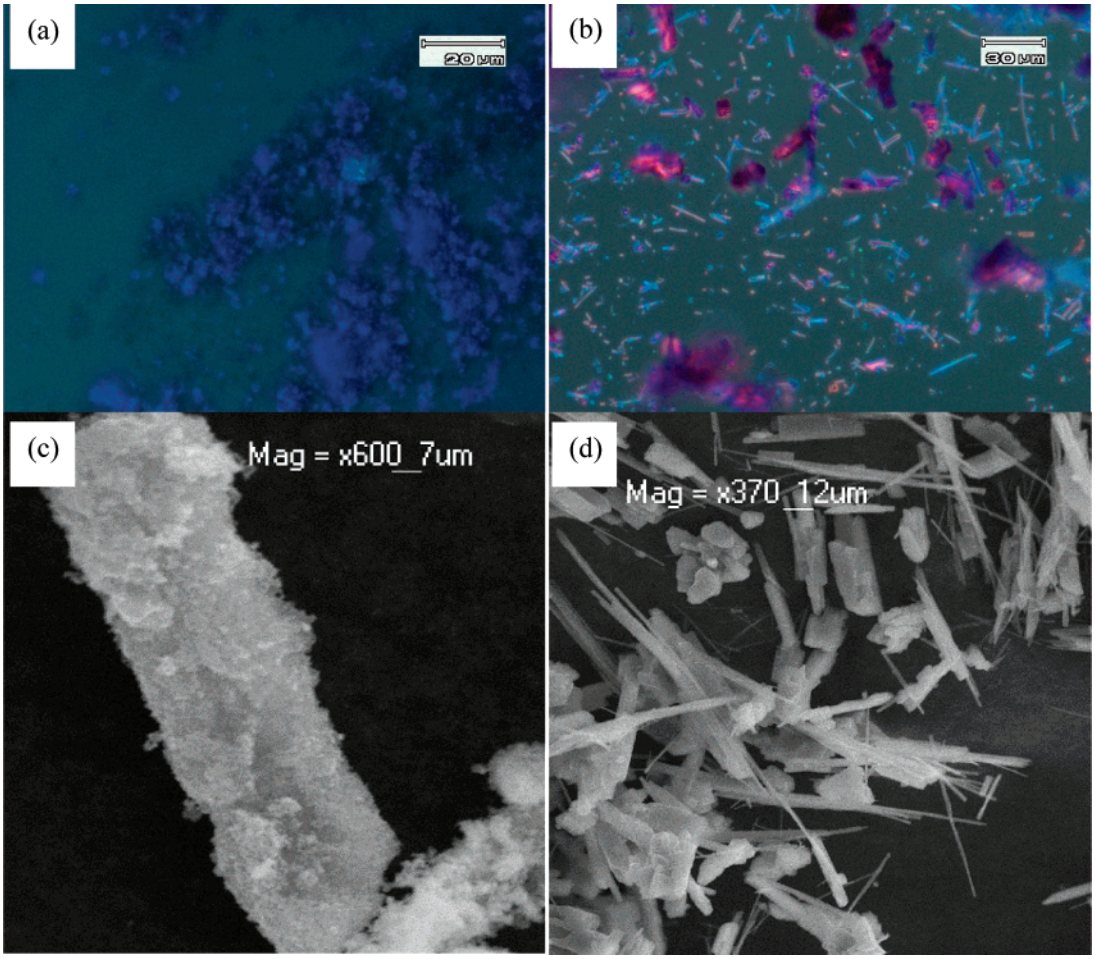

Figure 1. Images of chemically synthesized AgTCNQ (a and c) blue and (b and d) red forms obtained by SEM (c,d) and optical microscopy (a,b).

nanorods (Figure 1b and d). However, grinding either form to a submicron size produced blue powders, suggesting that detection of the red color in the needle shaped crystals is a direct consequence of this morphology and not because of phase differences. Further support for this conclusion is as follows: SECM approach curves for either solid adhered to glass in contact with aqueous ferrocenemethanol acting as a mediator were indistinguishable (distinctly different data were obtained from the two phases of CuTCNQ[23]); Raman and infrared spectra (Figures S1a and b, Supporting Information) are indistinguishable and in agreement with the literature;[19] DSC data collected over a temperature range of −150 to 370 °C revealed identical featureless behavior; powder XRD patterns of both forms are very similar (Figure S1c). The XRD result confirms that both samples are crystalline and most probably have the same crystal structure, even though the peak intensities for so-called phase I are lower than so-called phase II, due to a smaller amount of sample, and the ratios of peak heights are slightly different, which is considered most likely to be a result of a small amount of preferred orientation (not unreasonable given the high aspect ratio of the needle shaped red crystals). It was also found that a powder XRD pattern calculated from the single-crystal data[17] (Figure S1d) matches those obtained for blue and red forms of AgTCNQ.

Finally, it was found that the solubility of both AgTCNQ samples in acetonitrile was 0.15 ± 0.02 mM without electrolyte and 0.25 ± 0.02 mM with electrolyte (0.1 M Bu_4NBF_4). This equates to a solubility product (K_{sp}) of 2.2×10^{-8} M^2 without electrolyte and 6.2×10^{-8} M^2 with electrolyte, which is slightly smaller than the value of 4.9×10^{-7} M^2 for CuTCNQ in acetonitrile (0.1 M Bu_4NPF_6).[22]

Cyclic Voltammetry when $Ag^+_{(MeCN)}$ and $TCNQ_{(MeCN)}$ Are Individually Present in Acetonitrile. $TCNQ_{(MeCN)}$ undergoes two reversible reduction processes to form $TCNQ^{\bullet -}_{(MeCN)}$ and then $TCNQ^{2-}_{(MeCN)}$ at metal and GC electrodes (Figure 2a and eq 5).[22] The reversible potentials are 230 and −310 mV respectively (all potentials are vs Ag/AgCl). $Ag^+_{(MeCN)}$ undergoes reduction in acetonitrile to form $Ag_{(metal)}$ (Figure 2b and eq 3). Initially, scanning in the negative potential direction generates a reduction peak at −65 mV (scan rate = 20 mV s^{-1}). On reversing the potential direction, current crossovers occur at 60 mV and 260 mV, indicative of a silver nucleation and growth process (overpotential is required to induce nucleation). A sharp oxidative stripping peak is then detected at 510 mV. On subsequent cycles, the reduction peak potential shifts to 140 mV, due to $Ag_{(metal)}$ now present on the electrode, allowing a lower nucleation overpotential. Analogous behavior is seen for the reduction and stripping of $Ag_{(metal)}$ on a Pt electrode (Figure S2a, Supporting Information).

$$TCNQ_{(MeCN)} + e^- \rightleftharpoons TCNQ^{\bullet -}_{(MeCN)} + e^- \rightleftharpoons TCNQ^{2-}_{(MeCN)} \quad (5)$$

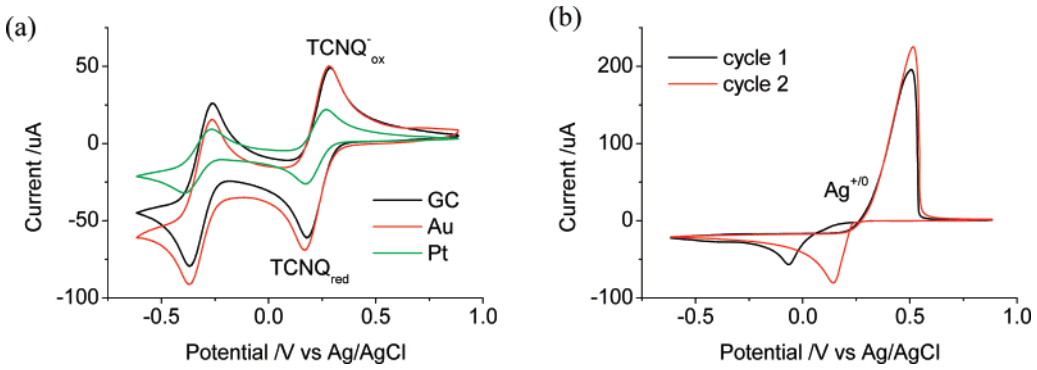

Figure 2. Cyclic voltammetry in acetonitrile (0.1 M Bu_4NBF_4) at a scan rate of 100 mV s^{-1}: (a) 10 mM $TCNQ_{(MeCN)}$ at a 1.5 mm diameter GC, 1.5 mm diameter gold, and 1 mm diameter platinum electrode and (b) 10 mM $Ag^+_{(MeCN)}$ at a 1.5 mm diameter GC electrode over two cycles of the potential.

Table 1. Reversible Potential Data ($E^{\circ\prime}$) for TCNQ and Silver in Water and Acetonitrile

reaction	$E^{\circ\prime}$ vs SCE (V)
$Ag^+_{(aq)} + e^- \rightleftharpoons Ag_{(s)}$	0.557[a]
$TCNQ_{(aq)} + e^- \rightleftharpoons TCNQ^{\bullet-}_{(aq)}$	0.115[b]
$TCNQ^{\bullet-}_{(aq)} + e^- \rightleftharpoons TCNQ^{2-}_{(aq)}$	−0.128[b]
$Ag^+_{(MeCN)} + e^- \rightleftharpoons Ag_{(s)}$	0.318[c]
$TCNQ_{(MeCN)} + e^- \rightleftharpoons TCNQ^{\bullet-}_{(MeCN)}$	0.21[d]
$TCNQ^{\bullet-}_{(MeCN)} + e^- \rightleftharpoons TCNQ^{2-}_{(MeCN)}$	−0.33[d]

[a] Reference 30. [b] 0.1 M $LiClO_4$.[31] [c] Reference 32. [d] 0.1 M Bu_4NPF_6.[33]

The thermodynamic standard potential data for the reduction of $TCNQ_{(MeCN)}$ and $Ag^+_{(MeCN)}$ (Table 1) suggest that $Ag_{(metal)}$ deposition could occur prior to $TCNQ_{(MeCN)}$ reduction. However, inspection of individual voltammograms for the $TCNQ^{0/\bullet-}$ and $Ag^{+/0}$ reduction processes at a GC electrode reveals that the slow kinetics for $Ag_{(metal)}$ deposition provides a small potential region where $TCNQ^{\bullet-}_{(MeCN)}$ may be formed in the presence of $Ag^+_{(MeCN)}$. This meets the required condition where reduction of $TCNQ_{(MeCN)}$ to $TCNQ^{\bullet-}_{(MeCN)}$ takes place at potentials less negative than $Ag^+_{(MeCN)}$ reduction to enable the generation of AgTCNQ to occur via eqs 1 and 2. Nevertheless, application of a sufficiently negative potential will generate $Ag_{(metal)}$. Since neutral $TCNQ_{(MeCN)}$ is still present in bulk solution, AgTCNQ also may be generated via eqs 3 and 4, but only simultaneously with material produced via eqs 1 and 2. In contrast, on a gold electrode (Figure S2a), the $Ag_{(metal)}$ deposition occurs at a less negative (220 mV) potential than on GC and Pt[29] and hence prior to the onset of the $TCNQ^{0/\bullet-}$ process. This reversal of order of potential restricts access to the electrocrystallization of AgTCNQ using a gold electrode via eqs 3 and 4.

Cyclic Voltammetric Reduction of $TCNQ_{(MeCN)}$ in Acetonitrile in the Presence of $Ag^+_{(MeCN)}$. When both 3.2 mM $Ag^+_{(MeCN)}$ and 9.6 mM $TCNQ_{(MeCN)}$ are present in acetonitrile (0.1 M Bu_4NBF_4), cyclic voltammograms at a scan rate of 20 mV s^{-1} on a GC electrode show that current arising from reduction of $TCNQ_{(MeCN)}$ begins at around 360 mV, as in the case in the absence of $Ag^+_{(MeCN)}$. However, at approximately 290 mV, the reductive current now increases very rapidly (labeled I_{red} in Figure 3a). On reversing the scan direction at 285 mV, the current continues to increase until a maximum value of −58 μA is reached at 290 mV, after which rapid decay of current occurs at even more positive potentials. Current crossover with the forward scan is now detected at 360 mV, which is indicative of nucleation and growth of a solid other than $Ag_{(metal)}$ on the electrode surface. At even more positive potentials, a sharp oxidation peak at 420 mV (labeled I'_{strip}) is followed by a second broader oxidation process at 670 mV (labeled I''_{strip}). Detection of a nucleation and growth process, commencing at potentials less negative than where reduction of $Ag^+_{(MeCN)}$ to $Ag_{(metal)}$ occurs at the bare electrode, implies that electrocrystallization of AgTCNQ can occur via reduction of $TCNQ_{(MeCN)}$ to $TCNQ^{\bullet-}_{(MeCN)}$ in the presence of $Ag^+_{(MeCN)}$ (eqs 1 and 2) in an analogous manner to the formation of CuTCNQ by reduction of $TCNQ_{(MeCN)}$ in the presence of $Cu^+_{(MeCN)}$.[22] Furthermore, it seems that oxidation of AgTCNQ back to $Ag^+_{(MeCN)}$ and $TCNQ_{(MeCN)}$ occurs via two mechanisms, whereas only one process was seen for the stripping of CuTCNQ to $Cu^+_{(MeCN)}$ and $TCNQ_{(MeCN)}$.

When the concentrations of both $Ag^+_{(MeCN)}$ and $TCNQ_{(MeCN)}$ are 9.1 mM, the current magnitudes for all processes increase (Figure 3a). On second and subsequent cycles of the potential (Figure 3b), the reductive current I_{red} increases even more rapidly when the potential reaches that needed for $TCNQ_{(MeCN)}$ reduction. If all AgTCNQ is not removed during the assumed stripping processes, AgTCNQ growth can occur on the residual crystals in repetitive potential cycling experiments. The crossover potential remains essentially the same on each cycle of the potential, but the current magnitudes for both I'_{strip} and I''_{strip} processes progressively get smaller, which may be due to a small level of dissolution of AgTCNQ, but is more likely as a result of only a moderate level of conductivity of AgTCNQ, restricting the amount of this solid stripped from the electrode.

If the switching potential is extended to 185 mV, the initially detected reduction current still increases rapidly at the onset of the $TCNQ_{(MeCN)} \rightarrow TCNQ^{\bullet-}_{(MeCN)}$ process, but now a peak exhibiting a diffusion-controlled tail is detected at 270 mV (labeled $I_{red} + II_{red}$ in Figure 3c). On switching the potential and scanning in the positive direction, the I'_{strip} and I''_{strip} processes shift to more positive potentials and the

(29) Vinokur, N.; Miller, B.; Avyigal, Y.; Kalish, R. *J. Electrochem. Soc.* **1999**, *146*, 125−130.
(30) Bard, A. J.; Faulkner, L. R., *Electrochemical Methods*, 2nd ed.; Wiley: New York, 2001.
(31) Sharp, M. *Anal. Chim. Acta* **1976**, *85*, 17−30.
(32) Marcus, Y. *Pure Appl. Chem.* **1985**, *57*, 1129−1132.
(33) Oyama, M.; Webster, R. D.; Suarez, M.; Marken, F.; Compton, R. G.; Okazaki, S. *J. Phys. Chem. B* **1998**, *102*, 6588−6595.

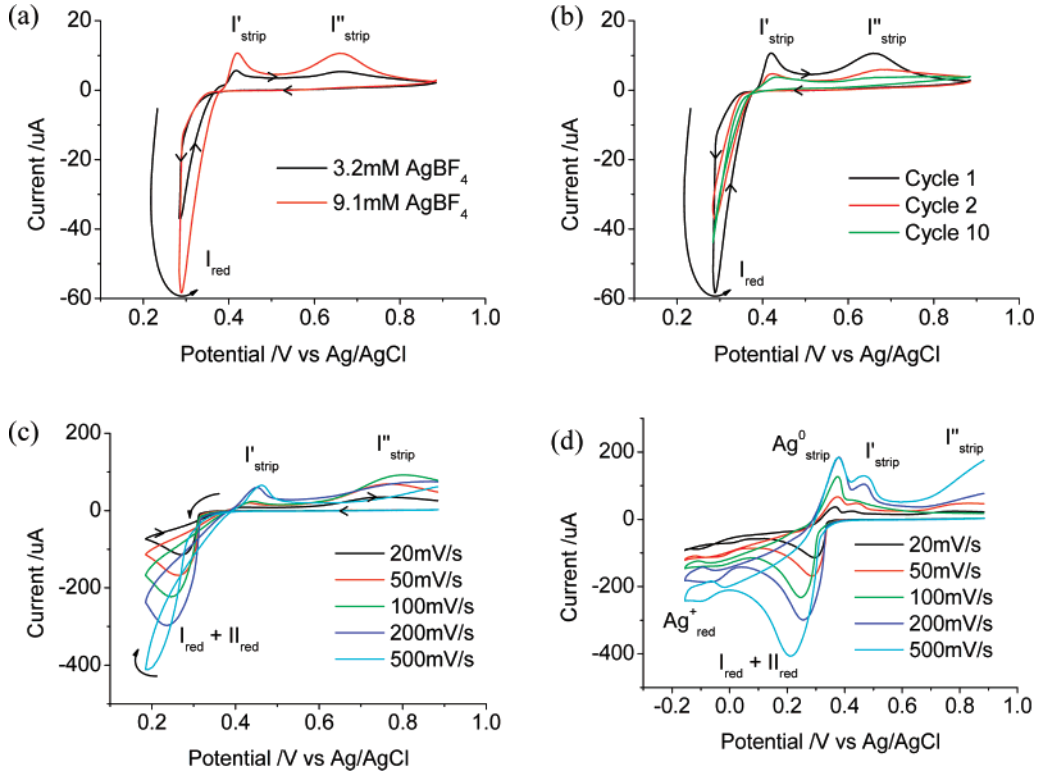

Figure 3. Cyclic voltammetry in acetonitrile (0.1 M Bu_4NBF_4) beginning at 885 mV (a−d) at a 3 mm diameter GC electrode for (a) ~9 mM $TCNQ_{(MeCN)}$ at a scan rate of 20 mV s^{-1} in the presence of a variable $Ag^+_{(MeCN)}$ concentration and with a switching potential of 283 mV, (b) equimolar 9.1 mM $TCNQ_{(MeCN)}$ and $Ag^+_{(MeCN)}$ at a scan rate of 20 mV s^{-1} for potential cycles 1, 2, and 3 with a switching potential of 283 mV, (c) equimolar 9.1 mM $TCNQ_{(MeCN)}$ and $Ag^+_{(MeCN)}$ at varying scan rates with a switching potential of 185 mV, and (d) equimolar 9.1 mM $TCNQ_{(MeCN)}$ and $Ag^+_{(MeCN)}$ at varying scan rates with a switching potential of −155 mV.

I'_{strip} peak height is now smaller than I''_{strip}, which represents the reverse situation prevailing when the switching potential is set at 285 mV.

Increasing the scan rate from 20 to 50, 100, and 200 mV s^{-1} (Figure 3c) leads to the reductive current just prior to the switching potential, increasing linearly with the square root of the scan rate, indicating diffusion control, while the magnitudes of both oxidation processes from the reverse scan also increase. At a scan rate of 500 mV s^{-1} the I_{red} + II_{red} process shifts to significantly more negative potentials, as the electrocrystallization process is beginning to be outrun.

When the switching potential is set at an even more negative potential of −155 mV (Figure 3d), a third small reduction process is detected at around −100 mV as is a new sharp oxidation process at 380 mV on the reverse scan along with the two AgTCNQ oxidation processes noted previously. The new reduction and oxidation processes occur at potentials close to where reduction of $Ag^+_{(MeCN)}$ and stripping of $Ag_{(metal)}$ occur at a bare GC electrode. This is probably attributed to residual $Ag^+_{(MeCN)}$ available as a result of the slight solubility of AgTCNQ in acetonitrile.

Oxidation of Electrocrystallized Samples of AgTCNQ. An equimolar solution of 9.1 mM $TCNQ_{(MeCN)}$ and $Ag^+_{(MeCN)}$ in acetonitrile (0.1 M Bu_4NBF_4) was subjected to reductive electrolysis at a GC electrode in order to induce AgTCNQ electrocrystallization. After electrocrystallization for 1 s at 285 mV (Figure 4a), followed by scanning the potential in the positive direction, an oxidation process in the potential region of process I'_{strip} is followed by a broader one in the I''_{strip} potential region. When the AgTCNQ deposition time is progressively increased to 2, 5, 10 and 30 s, the magnitudes of both I'_{strip} and I''_{strip} processes increase. Concomitantly, the ratio of the peak height of the I''_{strip} to the I'_{strip} process increases, and peak potentials shift (less positive potentials for I'_{strip}, more positive potentials for I''_{strip}). Stripping after deposition at the less positive potential of 185 mV (Figure 4b) was qualitatively similar, with the I''_{strip} process again being favored at longer deposition times. In contrast, use of a considerably more negative potential of −155 mV (Figure 5c) leads to dramatically different shaped stripping voltammetry. After 1 s deposition followed by scanning in the positive potential direction, two well-defined oxidation peaks at 350 and 480 mV attributed to Ag^0_{strip} and I'_{strip}, respectively, are evident, but with only a barely detectable response now found for process I''_{strip}. Increasing the deposition time favors the Ag^0_{strip} process over I'_{strip} and I''_{strip}, to the point when the latter are absent with deposition times of 10 s or longer.

The above series of deposition-stripping voltammetric experiments imply that electrocrystallized AgTCNQ is generated on the electrode surface when deposition occurs at potentials prior to reduction of $Ag^+_{(MeCN)}$ to $Ag_{(metal)}$. If the deposition potential is sufficiently negative and long times are used, extensive nucleation and growth of $Ag_{(metal)}$ restricts the extent of formation of AgTCNQ. However, in essence, it seems possible to detect two stripping potential regions for AgTCNQ and one for $Ag_{(metal)}$, with the relative importance being strongly dependent on the conditions employed.

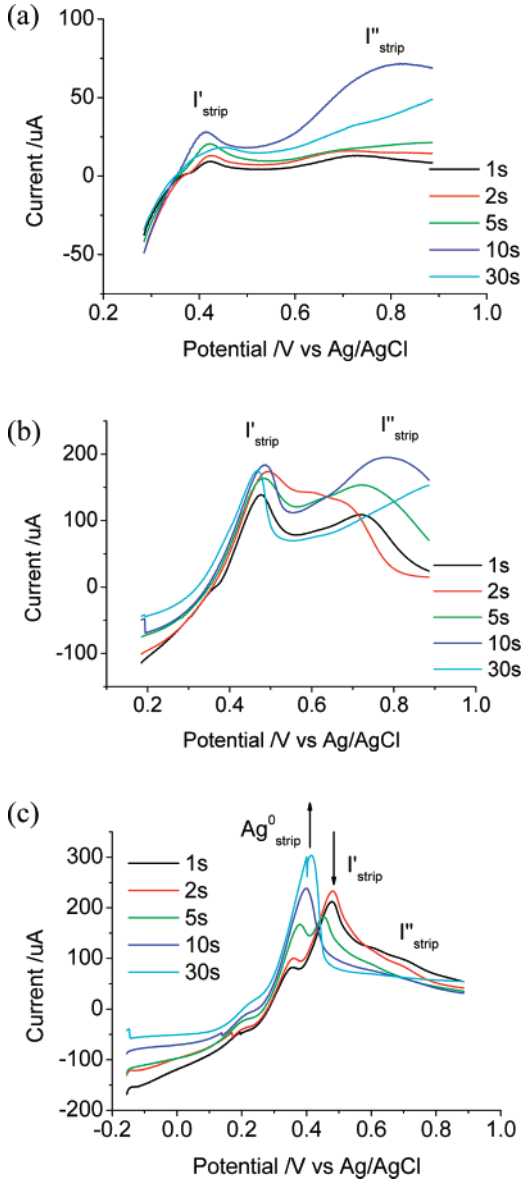

Figure 4. Stripping voltammetry from a solution containing equimolar 9.1 mM $TCNQ_{(MeCN)}$ and $Ag^{+}_{(MeCN)}$ in acetonitrile (0.1 M Bu_4NBF_4) at a 3 mm diameter GC electrode with a scan rate of 100 mV s^{-1} after electrocrystallization of AgTCNQ at deposition potentials of (a) 285, (b) 185, and (c) −155 mV.

Simultaneous Voltammetric and Surface Plasmon Resonance Studies at a Gold Electrode When $TCNQ_{(MeCN)}$ Is Reduced in the Presence and Absence of $Ag^{+}_{(MeCN)}$. Cyclic voltammograms obtained at a gold electrode with equimolar 9.1 mM $Ag^{+}_{(MeCN)}$ and $TCNQ_{(MeCN)}$ are distinctly different from those seen at a GC electrode (compare Figures 3d and S2b). In the case of gold, the $Ag_{(metal)}$ deposition and stripping processes are always dominant.

In situ voltammetric and surface plasmon resonance studies on gold electrodes can provide information on the AgTCNQ deposition and stripping processes. As shown previously,[25] cyclic voltammetry for 10 mM $TCNQ_{(MeCN)}$ in acetonitrile (0.1 M Bu_4NBF_4) gives rise to a reversible, sigmoidal decrease in SPR angle of 200 m° for the first $TCNQ^{0/\bullet-}$ process, and a reversible, sigmoidal increase of about 200 m° on the second $TCNQ^{\bullet-/2-}$ process (Figure 5a). This SPR change was attributed to variations in the solution permittivity (which may depend on the molar extinction coefficient or refractive index of the solution) rather than interaction of TCNQ materials with the electrode surface. Achievement of reduction of 10 mM $Ag^{+}_{(MeCN)}$ in acetonitrile (0.1 M Bu_4NBF_4) by scanning the potential in the negative direction led to a small initial decrease in SPR angle of 15 m° (at −180 mV, all potentials in SPR studies are vs a Pt quasi-reference electrode rather than Ag/AgCl) followed by a large increase of 1430 m° up to the switching potential. This large increase in the SPR response is attributed to bulk $Ag_{(metal)}$ deposition onto the gold surface, which continues after switching and reversing the potential direction and only stops when stripping of $Ag_{(metal)}$ commences (Figure 5b). At sufficiently positive potentials in the reverse scan where the $Ag_{(metal)}$ stripping process is complete, the SPR angle reattains the baseline value.

Use of a 3.2 mM $Ag^{+}_{(MeCN)}$−9.6 mM $TCNQ_{(MeCN)}$ solution (Figure 5c) provides voltammetric data similar to that found with a conventional planar disk gold electrode (compare Figures 5c and S2b). The SPR signal measured simultaneously as the potential is changed under conditions of cyclic voltammetry initially decreases sharply by 15 m°, as found for the pure $Ag^{+}_{(MeCN)}$ solution. As the potential is scanned negatively, a decrease of approximately 200 m° is seen, as is the case in the pure $TCNQ_{(MeCN)}$ solution. Reversing the scan direction returns the SPR signal to its initial value. These data imply that, on the reverse scan, $TCNQ^{\bullet-}_{(MeCN)}$ is oxidized back to $TCNQ_{(MeCN)}$ and $Ag_{(metal)}$ is stripped from the surface with little evidence for formation of surface confined AgTCNQ.

When 6.4 mM $Ag^{+}_{(MeCN)}$ is present (Figure 5d), the initial SPR angle decreases in response to the reduction of $TCNQ_{(MeCN)}$ to $TCNQ^{\bullet-}_{(MeCN)}$. The increase of 100 m° over the potential range of −300 mV to the switching potential of −500 mV is attributed to bulk $Ag_{(metal)}$ deposition. On reversing the potential scan direction, the SPR angle continues to increase at a rate that is enhanced by $TCNQ^{\bullet-}_{(MeCN)}$ oxidation back to $TCNQ_{(MeCN)}$. This is followed by a potential region where the SPR angle decreases by 100 m° due to $Ag_{(metal)}$ stripping. Over the potential range of −100 to −60 mV, $TCNQ^{\bullet-}_{(MeCN)}$ and $Ag^{+}_{(MeCN)}$ are both present at the electrode surface. The SPR signal increase of 15 m° in this range may indicate formation of AgTCNQ. As the potential becomes more positive, the SPR angle decreases as expected when the remaining $Ag_{(metal)}$ and AgTCNQ are stripped off the electrode.

At a high $Ag^{+}_{(MeCN)}$ concentration of 9.1 mM, the SPR angle initially decreases (Figure 5e) in response to the $TCNQ_{(MeCN)} \rightarrow TCNQ^{\bullet-}_{(MeCN)}$ process, which is followed by onset of bulk $Ag_{(metal)}$ deposition (signal increase of 900 m° over the potential range of −200 mV to the switching potential of −500 mV and also during the positive potential scan direction to −350 mV). Under these high $Ag^{+}_{(MeCN)}$ concentrations, no peak is detected in the SPR response from the $TCNQ^{\bullet-}_{(MeCN)} \rightarrow TCNQ_{(MeCN)}$ oxidation process, but the onset of the $Ag_{(metal)}$ stripping coincides with a sharp SPR signal loss until a potential of −40 mV is reached. The SPR angle now rises by 200 m°, over a very narrow potential range before rapidly returning to close to the baseline value at a potential of 20 mV. The now more obvious transient

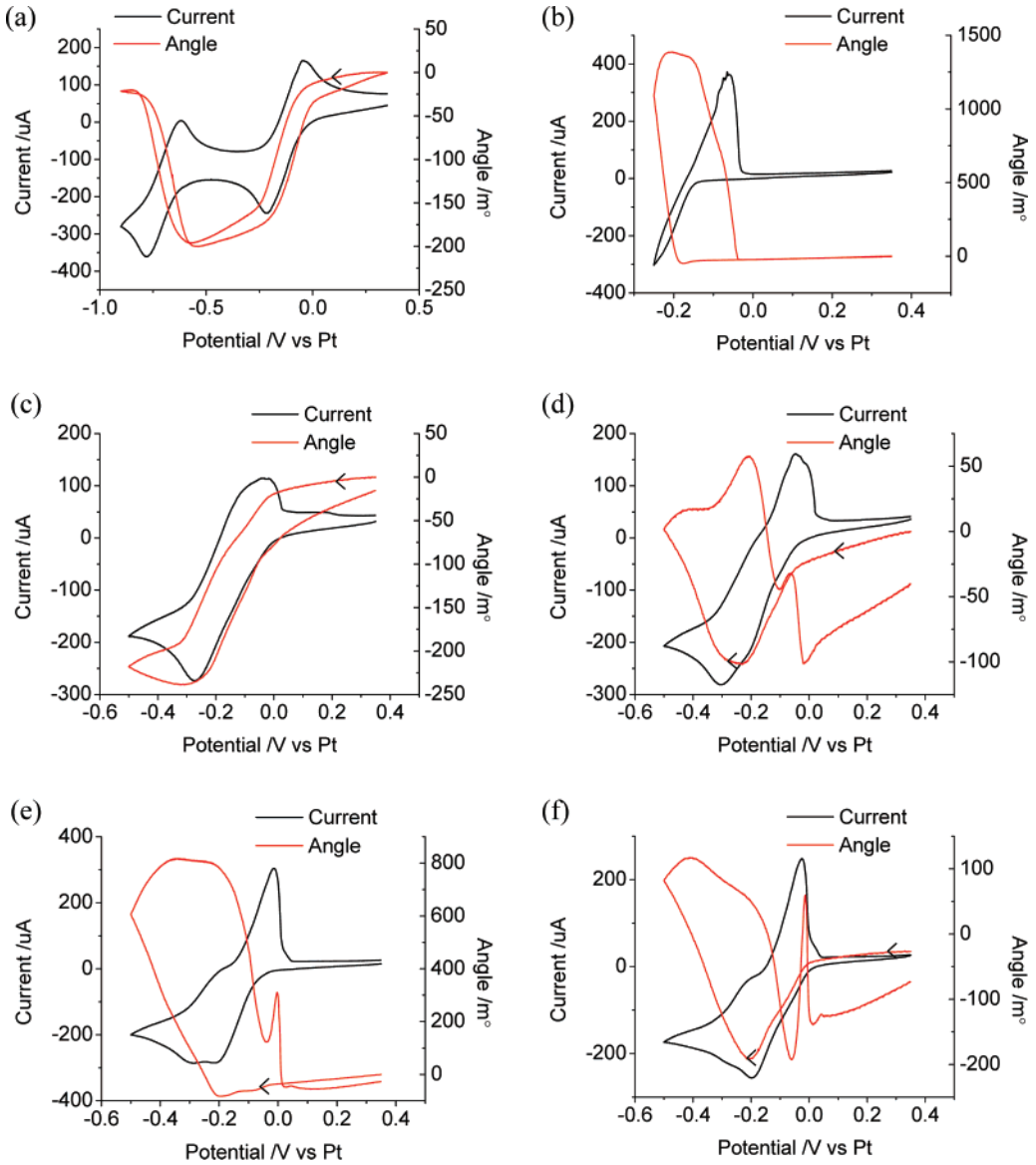

Figure 5. SPR data (current, black; SPR signal, red) obtained from a gold electrode in acetonitrile (0.1 M Bu_4NBF_4) using a scan rate of 100 mV s^{-1} with (a) 10 mM $TCNQ_{(MeCN)}$, (b) 10 mM $Ag^+_{(MeCN)}$, (c) 3.2 mM $Ag^+_{(MeCN)}$ and 9.6 mM $TCNQ_{(MeCN)}$, (d) 6.2 mM $Ag^+_{(MeCN)}$ and 9.4 mM $TCNQ_{(MeCN)}$, and 9.1 mM $Ag^+_{(MeCN)}$ and 9.1 mM $TCNQ_{(MeCN)}$ cycles (e) 1 and (f) 2.

SPR response at −40 to 20 mV on the reverse scan is attributed to the formation and removal of electrocrystallized AgTCNQ. This sharp transient signal is even more pronounced in the second potential cycle (Figure 5f), which is consistent with further growth and stripping of AgTCNQ in this potential region on previously nucleated crystals that were not fully removed at the end of the first cycle. Thus, even on gold electrodes, AgTCNQ is believed to electrocrystallize, according to SPR evidence.

Cyclic Voltammetry at TCNQ and AgTCNQ Modified Electrodes in Contact with Aqueous 0.1 M $AgNO_{3(aq)}$ Electrolyte. $TCNQ_{(s)}$ adhered to an electrode surface in contact with $Ag^+_{(aq)}$ may in principle undergo two different processes to form AgTCNQ, one due to intercalation of $Ag^+_{(aq)}$ ions as a counterion into reduced $TCNQ^{\bullet -}$ formed in the $TCNQ^{0/\bullet -}$ process (eq 6), the other from reduction of $Ag^+_{(aq)}$ to $Ag_{(metal)}$ and its subsequent reaction with $TCNQ_{(s)}$ (eqs 7 and 8). However, the standard potential of the $TCNQ^{0/\bullet -}$ process in water is considerably more negative than the $Ag^{+/0}$ process (Table 1), and so the intercalation mechanism is not likely to be available. At a scan rate of 20 mV s^{-1}, $Ag_{(metal)}$ deposition from 0.1 M $AgNO_{3(aq)}$ electrolyte onto a bare GC electrode begins at 470 mV (Figure 6a). If the potential is switched at 450 mV, a peak is detected at 470 mV, current crossing at 510 mV, again indicative of a nucleation and growth mechanism, and $Ag_{(metal)}$ oxidative stripping occurs at 560 mV.

$$TCNQ_{(s)} + Ag^+_{(aq)} + e^- \rightleftharpoons [Ag^+TCNQ^{\bullet -}]_{(s)} \quad (6)$$

$$Ag^+_{(aq)} + e^- \rightleftharpoons Ag_{(metal)} \quad (7)$$

$$Ag_{(metal)} + TCNQ_{(s)} \rightleftharpoons [Ag^+TCNQ^{\bullet -}]_{(s)} \quad (8)$$

Electrochemical stripping can be detected when chemically synthesized blue AgTCNQ mechanically adhered to a GC electrode surface is placed in contact with 0.1 M $AgNO_{3(aq)}$, and the positive direction potential sweep is commenced at

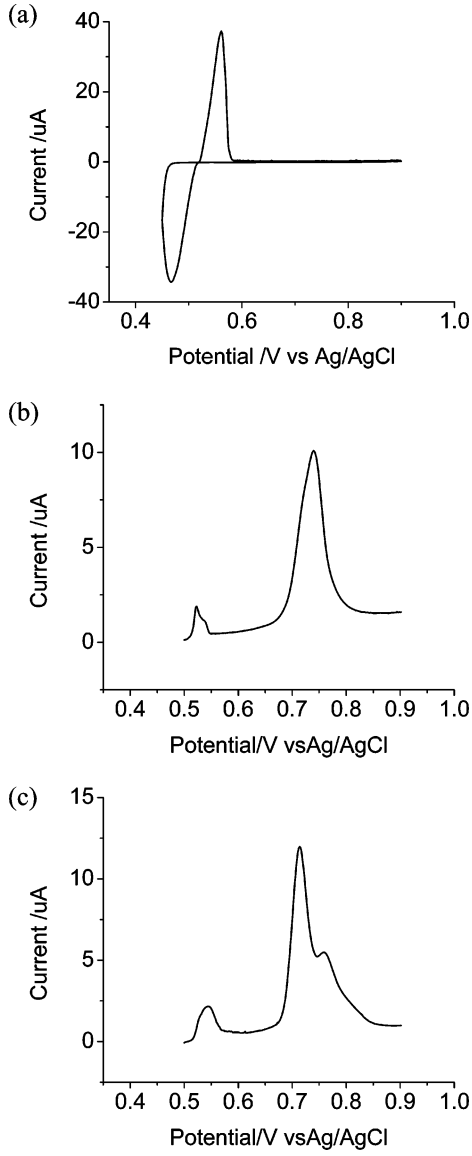

Figure 6. Cyclic voltammetry in water (0.1 $AgNO_{3(aq)}$) at a 3 mm diameter GC electrode at a scan rate of 20 mV s^{-1} for (a) deposition and stripping of $Ag_{(metal)}$, (b) stripping of AgTCNQ blue microcrystals, and (c) red needles.

510 mV (crossover potential for the $Ag_{(metal)}$ deposition/stripping process) (Figure 6b). Specifically, scanning in the positive potential direction produced a very small oxidation peak at 520 mV (same potential region as the Ag^0_{strip} process in 0.1 M $AgNO_{3(aq)}$ or I'_{strip} in acetonitrile, assuming that reference electrode junction potentials in acetonitrile are small) followed by a broad stripping peak at 740 mV which has a shoulder at 720 mV (in the same potential region as process I''_{strip} in acetonitrile). Stripping of chemically synthesized red AgTCNQ mechanically adhered to the electrode surface is associated with a small oxidation peak at 540 mV, and two resolved stripping peaks at 710 and 760 mV (Figure 6c).

Voltammograms obtained when a drop cast $TCNQ_{(s)}$ modified GC electrode is placed in 0.1 M $AgNO_{3(aq)}$ exhibit the expected $Ag_{(metal)}$ deposition and stripping process (Figure S3a, Supporting Information, and eq 7). However, on reversing the direction of the scan toward the initial potential, detection of a broad symmetrical oxidation process resembles that found from stripping of blue AgTCNQ (formed via eq 8). On the second cycle of the potential, this stripping peak is detected at 710 mV as would be expected if red AgTCNQ were formed. Cyclic voltammetry with mechanically adhered $TCNQ_{(s)}$ (Figure S3b) is similar to that found with drop cast $TCNQ_{(s)}$, although a larger AgTCNQ stripping peak appears at 690 mV on the first potential cycle. On cycling the potential, the stripping peak occurs at 710 mV on the second cycle and 720 mV on the tenth cycle, implying conversion of the red to the blue forms of AgTCNQ.

Finally in this series of experiments, AgTCNQ was electrocrystallized onto a GC electrode from an equimolar solution of 9.1 mM $Ag^+_{(MeCN)}$ and $TCNQ_{(MeCN)}$ in acetonitrile (0.1 M Bu_4NBF_4) at a potential of 300 mV for 30 s or −100 mV for 1 s. The former experiment is believed to generate red and blue forms of AgTCNQ (Figure 4a) and the latter mainly the red crystal form of AgTCNQ (Figure 4c). The electrode was then carefully removed from the solution, and 3 drops of acetonitrile was then applied gently to the electrode surface before subsequent removal with a tissue to remove unreacted TCNQ, Ag^+, and electrolyte that would otherwise be retained on the electrode surface when the solvent evaporated. The AgTCNQ modified electrode was then placed into an aqueous (0.1 M $AgNO_{3(aq)}$) solution. AgTCNQ deposited at 300 mV from acetonitrile showed a sharp single stripping peak at 750 mV whereas AgTCNQ deposited at −100 mV generated an even larger stripping peak at 740 mV (Figure S3c). The stripping peaks found in these experiments are sharper and occur slightly more positive than found from chemically synthesized materials, implying that the stripping potential is very sensitive to the source of adhered AgTCNQ.

Examination of Electrocrystallized AgTCNQ by Microscopy, Spectroscopy, and Powder XRD. All electrocrystallized samples showed the expected presence of Ag, C, and N by EDAX and infrared absorptions and powder XRD patterns (Figure S1c) expected for AgTCNQ. Thus, distinctions by only electrochemistry, morphology, and color have been achieved.

SEM images of AgTCNQ electrocrystallized onto a GC electrode from an equimolar mixture of 9.1 mM $TCNQ_{(MeCN)}$ and $Ag^+_{(MeCN)}$ in acetonitrile (0.1 M Bu_4NBF_4) exhibited a large number of needles when the potential was held at 240 mV (I_{red}) for 30 s (Figure 7a). Electrocrystallization at the more negative potential of −100 mV ($I_{red} + II_{red}$) for 30 s (Figure 7b) also produced needles as well as much larger crystals, up to 100 μm in length and 20 μm in width. Finally, linear sweep voltammetry over the potential range of 800 mV to −100 mV at a scan rate of 100 mV s^{-1} generated a dense film of extremely high aspect ratio needles (Figure 7c).

The color of electrocrystallized AgTCNQ material formed as a function of experimental conditions was assessed by optical microscopy. When $Ag_{(metal)}$ was deposited at −100 mV for 10 s from 10 mM $Ag^+_{(MeCN)}$ in acetonitrile (0.1 M Bu_4NBF_4), and the rinsed electrode placed in 10 mM $TCNQ_{(MeCN)}$ for 30 s (Figure 8a), red needles were detected along with a small amount of residual $Ag_{(metal)}$. A further 60 s contact with 10 mM $TCNQ_{(MeCN)}$ (Figure S4a, Supporting Information) resulted in all of the $Ag_{(metal)}$ being incorporated

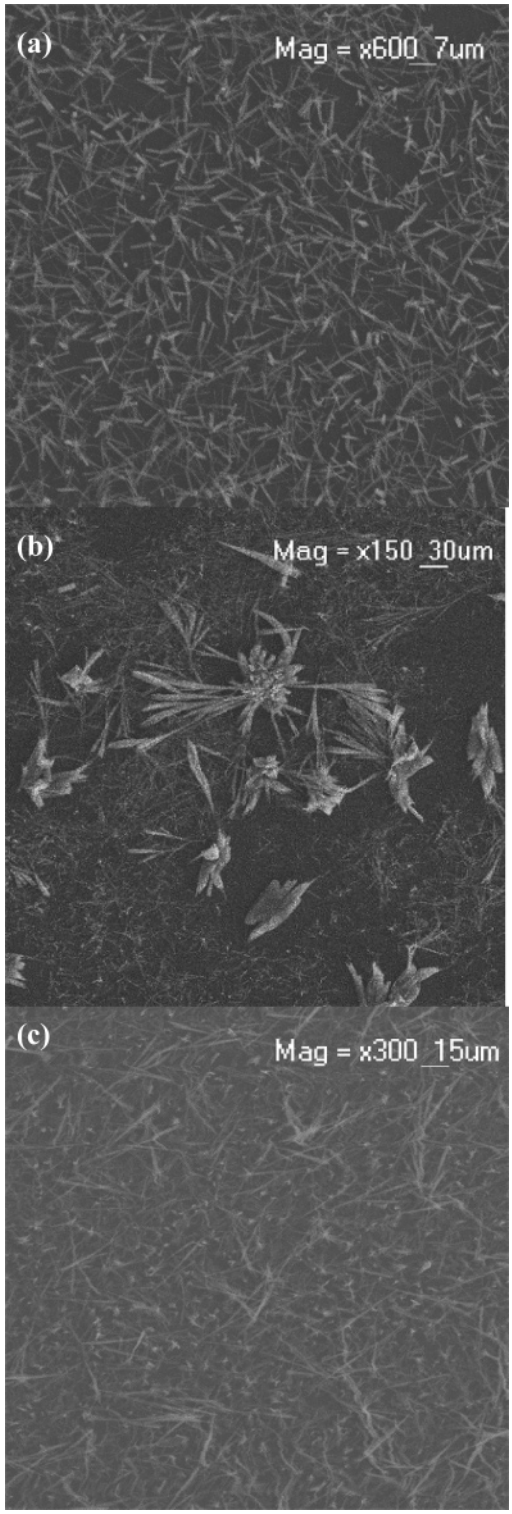

Figure 7. SEM images of AgTCNQ obtained from equimolar 9.1 mM $TCNQ_{(MeCN)}$ and $Ag^{+}_{(MeCN)}$ in acetonitrile (0.1 M Bu_4NBF_4) by electrocrystallization onto a 3 mm diameter GC electrode when the potential is held at (a) 240 mV for 30 s, (b) −100 mV for 30 s, and (c) from linear sweep voltammetry over the potential range of 800 to −100 mV at a scan rate of 100 mV s^{-1}.

into even larger red needles. The formation of AgTCNQ red needles, so-called phase II, by reaction of $Ag_{(metal)}$ and $TCNQ_{(MeCN)}$ is consistent with the previously reported data.[20]

AgTCNQ electrocrystallized onto a GC electrode at 300 mV (I_{red}) for 10 s from equimolar 9.1 mM $TCNQ_{(MeCN)}$ and $Ag^{+}_{(MeCN)}$ in acetonitrile (0.1 M Bu_4NBF_4) (Figure 8b) produces red needles and nanowires. In contrast, electrocrystallization at 0 V (I_{red} + II_{red}) for 10 s gives rise to a blue film morphology that coats the entire electrode surface (Figure 8c). However, close inspection of the image reveals that the blue film overlays red needles. If electrocrystallization is attempted at −100 mV (I_{red} + II_{red} + Ag^{+}_{red}) for 120 s (Figure 8d), $Ag_{(metal)}$ is formed on the electrode surface, while some red needles are present at the center of the electrode and blue film coated red needles are present at the electrode edge. Linear sweep voltammetry at a scan rate of 100 mV s^{-1} over the potential range of 1.1 to 0 V generates a dense film of red needles (Figure S4b). A cyclic voltammogram from 1.1 V to −300 mV and back to 1.1 V produced red needles coated with a blue film. Clearly some AgTCNQ remains adhered to the electrode surface (Figure S4c) despite the presence of a stripping peak in the voltammogram.

Similar images were obtained from AgTCNQ electrocrystallized on gold and indium tin oxide (ITO) electrodes. However, it was harder to control the crystal morphology on gold due to the more positive $Ag^{+}_{(MeCN)}$ reduction potential while on ITO, thick, weakly adhered films of AgTCNQ hindered rinsing and characterization.

Voltammetry with a $TCNQ_{(s)}$ modified electrode in contact with aqueous 0.1 M $AgNO_{3(aq)}$ indicated that both colors of AgTCNQ are formed as well as $Ag_{(metal)}$, as confirmed by examination of images obtained by optical microscopy (Figures 8e,f and S4d).

Mechanistic Considerations on the Formation of AgTCNQ. The mechanism of electrocrystallization of AgTCNQ is complex. The formation of arrays of red needles of AgTCNQ is favored by electrolysis at less negative potentials (process I_{red}) and for short time periods, when $TCNQ_{(MeCN)}$ is reduced to $TCNQ^{\bullet -}_{(MeCN)}$ in the presence of $Ag^{+}_{(MeCN)}$. This is consistent with electrocrystallization of well-spaced needles of CuTCNQ and $Co(TCNQ)_2(H_2O)_2$ where nucleation occurs at defect sites on the electrode surface.[22,28] This suggests that high aspect ratio AgTCNQ red needles are formed when slow crystal growth is allowed to proceed along a preferred axis, which occurs when the concentration of dissolved $Ag^{+}_{(MeCN)}$ and $TCNQ^{\bullet -}_{(MeCN)}$ is low as is the case at well-spaced defect sites on electrode surfaces. Equations 1 and 2 are proposed for this electrocrystallization process.

After longer periods of electrolysis or when the potential is held at slightly more negative potentials (process II_{red}), a blue film is generated over all areas of the electrode. This film morphology is similar to that found when CuTCNQ and $Co(TCNQ)_2(H_2O)_2$ produced via a well-resolved Faradaic process that occurs at more negative potentials in these systems.[25,28] By analogy it is postulated that, following the reduction of $TCNQ_{(MeCN)}$ to $TCNQ^{\bullet -}_{(MeCN)}$ (eq 1), the soluble metal ion stabilized $(TCNQ^{\bullet -})(TCNQ)$ dimer anion $Ag^{+}[(TCNQ^{\bullet -})(TCNQ)]_{(MeCN)}$ is formed (eq 9). $Ag^{+}[(TCNQ^{\bullet -})(TCNQ)]_{(MeCN)}$ is then reduced (eq 10) to produce the same crystals as formed via eqs 1 and 2, but nucleation and growth now occurs on all areas of the electrode surface to produce the blue film. No resolved second Faradaic process is detectable in the present case which implies that the potentials for reduction of $Ag^{+}[(TCNQ^{\bullet -})(TCNQ)]_{(MeCN)}$ and $TCNQ_{(MeCN)}$ are similar.

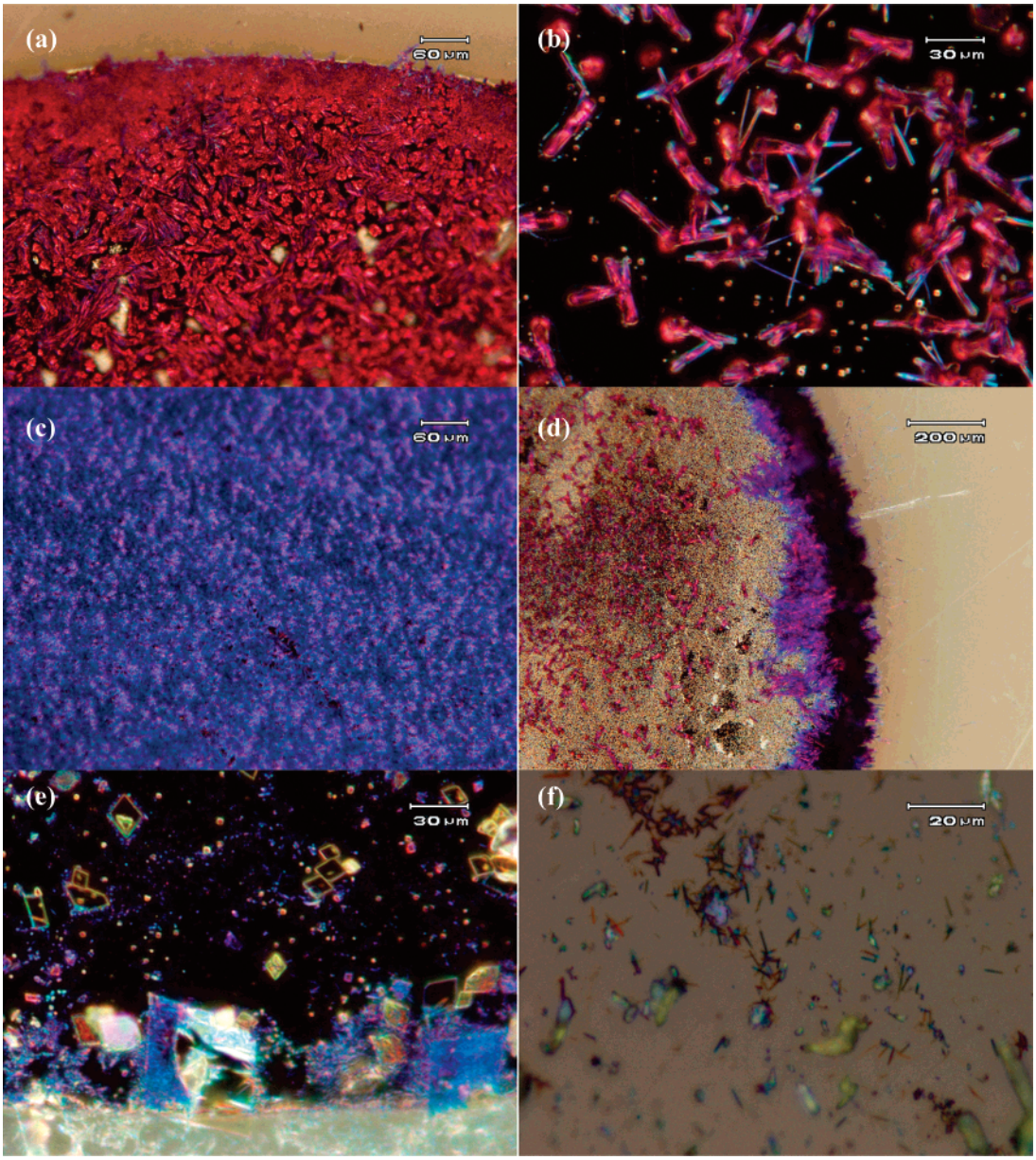

Figure 8. Optical microscopy of AgTCNQ generated on a 3 mm diameter GC electrode: (a) $Ag_{(metal)}$ deposited from 10 mM $Ag^{+}_{(MeCN)}$ in acetonitrile (0.1 M Bu_4NBF_4) at −100 mV for 10 s, rinsed in acetonitrile and placed in 10 mM $TCNQ_{(MeCN)}$ for 30 s; (b−d) electrocrystallized from equimolar 9.1 mM $TCNQ_{(MeCN)}$ and $Ag^{+}_{(MeCN)}$ in acetonitrile (0.1 M Bu_4NBF_4) at (b) 300 mV for 10 s, (c) 0 V for 10 s, and (d) −100 mV for 120 s; (e, f) in 0.1 M $AgNO_{3(aq)}$ via (e) reduction of a drop cast $TCNQ_{(s)}$ modified electrode at 400 mV for 30 s and (f) after 10.5 cycles of the potential over the range of 900 to 400 mV.

The appearance of the blue film only after long periods of time or at more negative potentials suggests that high concentrations of $TCNQ^{\bullet -}_{(MeCN)}$ are required for the formation of $Ag^{+}[(TCNQ^{\bullet -})(TCNQ)]_{(MeCN)}$. The synthetic route

$$Ag^{+}_{(MeCN)} + TCNQ_{(MeCN)} + TCNQ^{\bullet -}_{(MeCN)} \rightleftharpoons Ag^{+}[(TCNQ^{\bullet -})(TCNQ)]_{(MeCN)} \quad (9)$$

$$Ag^{+}[(TCNQ^{\bullet -})(TCNQ)]_{(MeCN)} + e^{-} \underset{\text{precipitation}}{\rightleftharpoons} [Ag^{+}TCNQ^{\bullet -}]_{(s)} + TCNQ^{\bullet -}_{(MeCN)} \quad (10)$$

to blue AgTCNQ also occurs when high concentrations of $Ag^{+}_{(MeCN)}$ and $TCNQ^{\bullet -}_{(MeCN)}$ are mixed together in acetonitrile, forcing rapid precipitation of the microcrystalline form and perhaps facilitating charge transfer between some Ag^{+} and $TCNQ^{\bullet -}$.

At even more negative potentials on a GC electrode, both $Ag^{+}_{(MeCN)}$ and $TCNQ_{(MeCN)}$ are reduced to $Ag_{(metal)}$ (eq 3) and $TCNQ^{\bullet -}_{(MeCN)}$ (eq 1). This inhibits electrocrystallization of AgTCNQ via eqs 1 and 2, while the absence of $Ag^{+}_{(MeCN)}$ prevents stabilization of $(TCNQ^{\bullet -})(TCNQ)$ dimer anions, and hence electrocrystallization via eqs 9 and 10.

Red needles of AgTCNQ also have been observed from reaction of $Ag_{(metal)}$ with $TCNQ_{(MeCN)}$ in acetonitrile, when $Ag_{(metal)}$ is deposited onto an electrode surface and then placed into a solution of $TCNQ_{(MeCN)}$ and when blue AgTCNQ is refluxed in acetonitrile for several days.

In aqueous 0.1 M $AgNO_{3(aq)}$, blue and red AgTCNQ are formed from the reduction of $TCNQ_{(s)}$. In this situation, AgTCNQ is produced by an electron transfer reaction between $Ag_{(metal)}$ and $TCNQ_{(s)}$ (eqs 7 and 8). AgTCNQ is practically insoluble in water and is unlikely to rearrange

along a preferred crystal axis, and its low conductivity limits the extent of AgTCNQ acting as an electrode for further AgTCNQ growth.

Conclusions

AgTCNQ may be synthesized in two different shaped and colored crystalline forms. However, the crystal structure and spectroscopic properties of the two forms appear to be identical and hence potentially are the same phase. Reduction of $TCNQ_{(MeCN)}$ in the presence of $Ag^{+}_{(MeCN)}$ at GC, Pt, and ITO electrodes electrocrystallizes either of the AgTCNQ morphologies. At minimum possible deposition potentials, the concentration of $TCNQ^{\bullet -}_{(MeCN)}$ at the electrode surface is low, allowing slow growth of high aspect ratio, red needle AgTCNQ crystals at well-spaced defect sites present on electrode surfaces. After longer periods and at more negative deposition potentials, the higher concentration of $TCNQ^{\bullet -}_{(MeCN)}$ favors faster growth of smaller crystals via reduction of $Ag^{+}[(TCNQ^{\bullet -})(TCNQ)]_{(MeCN)}$. This results in deposition of a blue microcrystalline AgTCNQ thin film over the red needles. At even more negative potentials, $Ag_{(metal)}$ nucleates, inhibiting growth of AgTCNQ. The effect of $TCNQ^{\bullet -}_{(MeCN)}$ concentration on crystal morphology of electrocrystallized material can be related to the chemical synthetic routes, where low concentrations of $Ag^{+}_{(MeCN)}$ and $TCNQ^{\bullet -}_{(MeCN)}$ produce red needles of AgTCNQ, as also is the case when $Ag_{(metal)}$ is placed into a solution of $TCNQ_{(MeCN)}$ and when blue microcrystalline AgTCNQ is refluxed in acetonitrile. In contrast, mixing high concentrations of $Ag^{+}_{(MeCN)}$ and $TCNQ^{\bullet -}_{(MeCN)}$ results in rapid precipitation of blue microcrystalline AgTCNQ. AgTCNQ can also form on a $TCNQ_{(s)}$ modified electrode in 0.1 M $AgNO_{3(aq)}$ where deposition of $Ag_{(metal)}$ onto the $TCNQ_{(s)}$ crystals allows a charge transfer process to occur. However, it is more difficult to control the morphology formed in this situation.

Acknowledgment. We would like to thank Rod Mackey and Dr. Craig Forsyth for help with collection and analysis of the powder XRD data and the Monash Electron Microscopy and Microanalysis Facility for access to their SEM facilities. A.R.H is also grateful for a grant provided by the American Electroplaters and Surface Finishers Society and a Monash University Postgraduate Publication Award in support of his work. A.M.B. expresses appreciation to the Australian Research Council for the award of a Federation Fellowship and to Monash University for financial support of this project.

Supporting Information Available: Figures S1−S4 (PDF): Raman and IR spectra and powder XRD of chemically synthesized AgTCNQ (Figure S1). Cyclic voltammetry at a gold electrode in acetonitrile (Figure S2) and at a chemically modified electrode in water (Figure S3). Optical microscopy of electrochemically synthesized AgTCNQ (Figure S4). This material is available free of charge via the Internet at http://pubs.acs.org.

CM070780B